Industrial Crops & Products 239 (2026) 122394

Contents lists available at ScienceDirect

Industrial Crops & Products

journal homepage: www.elsevier.com/locate/indcrop

Enzymatic dynamics and chemical transformation in *Dendrocalamus sinicus* biodeterioration by typical filamentous fungi

Jiyun Qi [a,d], Mizi Fan [b], Yonghui Zhou [b,c], Chen Zhang [d], Jialong Wen [d,*], Yan Xia [a,*]

[a] Yunnan Provincial Key Laboratory of Wood and Bamboo Biomass Materials, Southwest Forestry University, Kunming 650224, China
[b] College of Engineering, Design and Physical Sciences, Brunel University London, Uxbridge UB8 3PH, United Kingdom
[c] College of Materials and Energy, South China Agricultural University, Guangzhou 510642, China
[d] Beijing Key Laboratory of Lignocellulosic Chemistry, Beijing Forestry University, No. 35 Tsinghua East Road, Haidian District, Beijing 100083, China

ARTICLE INFO

Keywords:
Dendrocalamus sinicus
Biodeterioration
Enzymatic pathways
Chemical transformation
Bamboo protection

ABSTRACT

Dendrocalamus sinicus, the world's largest bamboo species, is valued for its high strength and rapid growth, finding extensive application in construction, furniture, and composite materials. However, mold-induced deterioration impairs the visual appearance, chemical stability, and structural integrity, thereby compromising service performance and lifespan. This study aimed to elucidate the multi-scale deterioration mechanisms of *Dendrocalamus sinicus* under colonization by *Aspergillus niger*, *Penicillium citrinum*, and *Trichoderma viride*. It was found that the deterioration efficiency depended critically on the spatiotemporal overlap between lignin-degrading enzyme and hydrolase activities. Hemicellulose was the primary and preferentially attacked component by all three molds. Distinct enzymatic pathways drive mold-specific cellulose-lignin biodeterioration. *Aspergillus niger* employed an inward-to-outward cellulose-prioritized pathway, *Penicillium citrinum* executed a surface-oriented lignin-prioritized degradation, and *Trichoderma viride* simultaneously decomposed cellulose and lignin. Microstructural erosion followed a continuous three-stage pattern commencing with colonization and consumption of readily decomposable substances, progressing to enzymatic deconstruction of cell walls, causing a sharp increase in porosity, and culminating in structural collapse. These mechanistic insights provide novel targets for developing species-tailored preservation technologies, which are essential for extending the service life of bamboo products and promoting the value-added conversion of bamboo resources within a circular economy framework.

1. Introduction

Amidst global forest resource depletion and sustainable development imperatives, bamboo has emerged as a strategic biomaterial for timber substitution due to its rapid growth cycle, high carbon sequestration efficiency, and renewability, playing a pivotal role in national resource security and low-carbon economies (Sun et al., 2011). Among diverse bamboo species, *Dendrocalamus sinicus* (*D. sinicus*) is distinguished by its exceptional physical properties, including heights up to 30 m and superior mechanical strength with a flexural strength exceeding 100 MPa (Xu et al., 2019). Chemically, it is characterized by a high holocellulose content (71.01 %), which comprises the total carbohydrate fraction of cellulose and hemicellulose, and a lignin content of 26.12 %, typical of grass-type lignins rich in guaiacyl (G), syringyl (S), and p-hydroxyphenyl (H) units (Fig. 1a) (Jiankun et al., 2019; Xiao et al., 2022; Yu and Wang, 2023). This unique physicochemical profile positions it as an ideal feedstock for engineered bamboo products and biorefineries. Nevertheless, industrial utilization of this species is severely constrained by pervasive mold colonization during processing and storage, leading to substantial material degradation and value depreciation (Chen et al., 2025a).

Aspergillus niger (*A. niger*), *Penicillium citrinum* (*P. citrinum*), and *Trichoderma viride* (*T. viride*) are established as primary mold agents responsible for bamboo deterioration, a process initiated by their colonization which primarily exploits non-structural nutrients in superficial layers as carbon sources (Bao et al., 2025). Through the secretion of extracellular enzymes, molds differentially degraded surface cellulose and lignin macromolecules, resulting in embrittlement and topographical roughening of the bamboo epidermis, the internal architecture remained largely intact, while substantial disagreement persisted

* Corresponding authors.
E-mail addresses: wenjialong@bjfu.edu.cn (J. Wen), xiayanswfu@gmail.com (Y. Xia).

https://doi.org/10.1016/j.indcrop.2025.122394
Received 20 August 2025; Received in revised form 3 November 2025; Accepted 25 November 2025
Available online 15 December 2025

regarding the extent of this degradation (Ma Xingxia, 2012). Although fungal degradation of bamboo components via secreted cellulases, hemicellulases, and lignin-modifying enzymes is recognized, fundamental knowledge gaps remain concerning the enzymatic synergy and species-specific degradation pathways in *D. sinicus*, including the spatiotemporal dynamics of enzyme secretion and the divergent depolymerization strategies employed by different molds (Saldarriaga-Hernández et al., 2020; Singh, 2021). Critically, the interface between enzymatic activity and chemical matrix deconstruction in mold-infested *D. sinicus* remains poorly understood, which impedes the development of targeted preservation strategies.

Currently, bamboo preservation primarily relies on conventional techniques such as broad-spectrum biocides and physical barriers. However, these methods are often associated with limitations including poor environmental compatibility, inadequate long-term efficacy, high economic costs, and the potential to induce microbial resistance (Lee et al., 2001). Existing anti-mold strategies are predominantly based on the macroscopic suppression of microbial growth, and lack systematic investigation into the degradation mechanisms of specific mold species at the molecular and biochemical levels. This gap in understanding species-specific degradation pathways and key functional targets prevents current technologies from achieving precise disruption of the biodeterioration process, thereby constraining their protective effectiveness and scope of application (Qi et al., 2022). Therefore, elucidating temporal patterns of enzyme secretion and concomitant physicochemical transformations during *D. sinicus* infestation by these molds will not

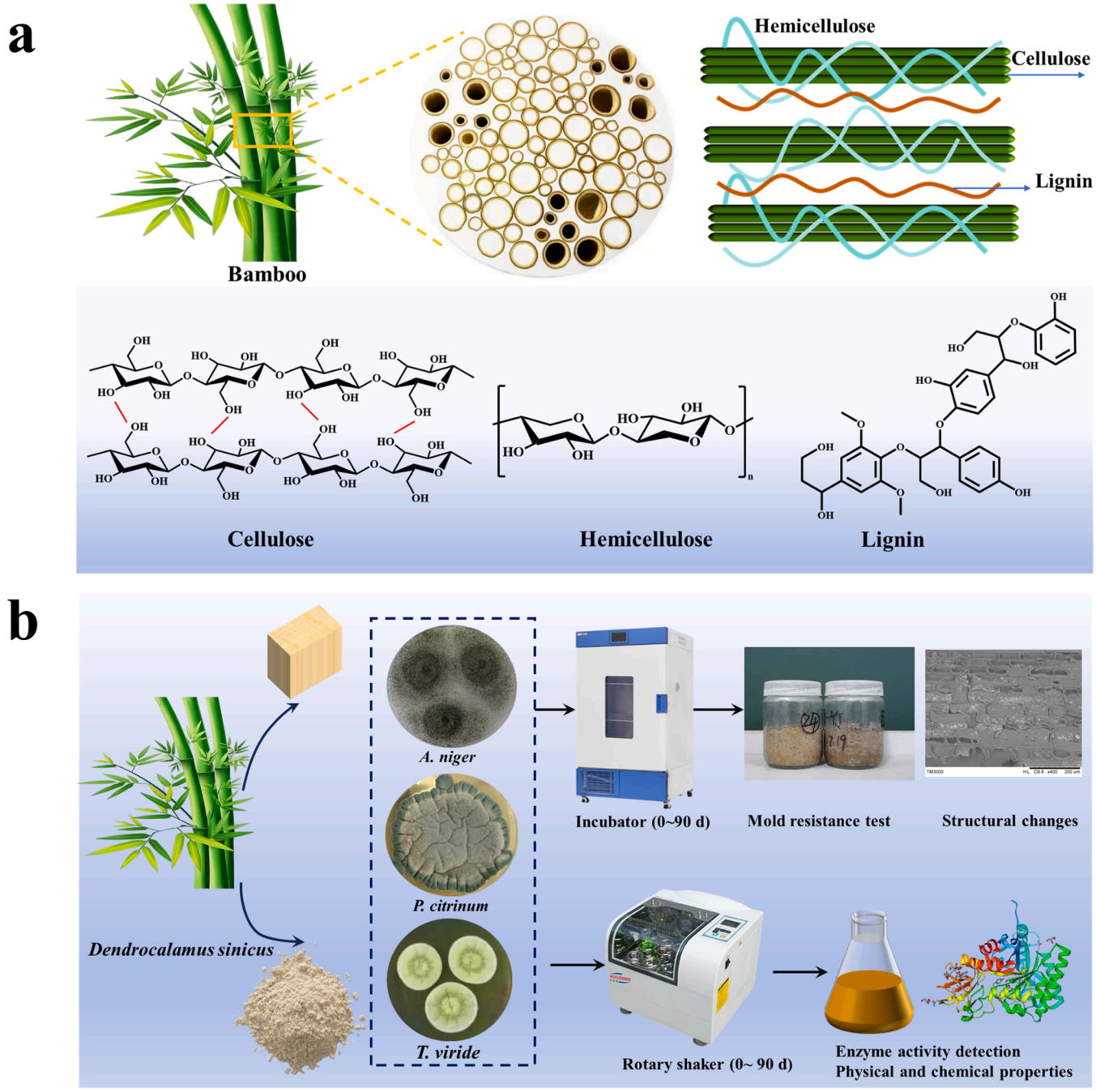

Fig. 1. Bamboo characterization and experimental scheme. (a) Microstructure and main chemical composition distribution of bamboo. (b) Schematic diagram of the experimental design and analytical procedure.

only elucidate molecular-scale biodeterioration mechanisms and advance multiscale decay theory, but also identify precision targets for customized preservation (e.g., suppressing *A. niger* cellulase expression or blocking *T. viride* metabolic pathways), thereby enabling sustainable bamboo biorefining.

This work deciphers the coevolutionary dynamics of fungal exoenzyme activity and substrate chemo-mechanics in *D. sinicus* under challenge by *A. niger*, *P. citrinum*, and *T. viride*. The study is driven by the need to clarify the enzymatic and physicochemical interactions that lead to material deterioration, which is essential for developing effective preservation methods and promoting the high-value utilization of *D. sinicus*. Specifically, the objectives of this study are to determine the spatiotemporal synergy thresholds of core enzymes such as cellulase, xylanase, and laccase that govern deterioration efficiency, and the strain-specific depolymerization strategies manifested through enzymatic portfolios, substrate preferences, and cooperative patterns (Fig. 1b). By mapping real-time interfacial responses in mold-bamboo systems, it provides a mechanistic foundation for countermeasure development and high-value utilization of *D. sinicus* resources.

2. Materials and methods

2.1. Materials

The 2-year-old *Dendrocalamus sinicus* (*D. sinicus*) samples, free of knots and no visible evidence of infection, were purchased from Dehong, Yunnan province, China. Before fungal conversion, all bamboo samples were dried at 103 ± 3 ℃ to a constant weight and the initial mass was recorded. The filamentous strains *A. niger*, *P. citrinum*, and *T. viride*, used in the mold erosion experiment, were provided by the China Forestry Culture Collection Center (CFCC).

2.2. Fungal processing

The *D. sinicus* powder (40–60 mesh) was used in the fungal cultivation experiments to maximize the interfacial contact area between the substrate and the filamentous strains, thereby enhancing fungal colonization and enzymatic degradation efficiency (Zhang et al., 2017a). The powder was mixed with sterile water at a ratio of 1:20 (w/v) in 250 mL Erlenmeyer flasks and sterilized by autoclaving at 121 °C for 1 h. After sterilization, each flask was inoculated with 10 fungal plugs (1 cm in diameter) of the respective filamentous strains and incubated in a rotary shaker at 30 °C and 180 rpm for 90 days. Supernatants were sampled every 10 days for enzyme activity assays. All enzyme activity measurements were carried out with three independent replicates, and the results are expressed as the mean ± standard deviation. In parallel, bamboo blocks measuring 2 × 2 × 1 cm were used for morphological observation according to the Chinese standard GB/T 29905 (2013). The same fungal strains were inoculated onto the block surfaces and incubated for 90 days. Samples were collected in triplicate ($n \geq 3$) at 30-day intervals (30, 60, and 90 days). After each sampling, surface mycelia were carefully removed, and the bamboo samples were dried at 103 ± 3 °C until constant weight was achieved. The mass loss was calculated using the following formula: Mass loss (%) = [(M_0 - Mt) / M_0] × 100. where M_0 represents the initial oven-dry mass (g) and Mt denotes the oven-dry mass (g) at day t (t = 30, 60, 90).

2.3. Enzymatic activities assay

Hydrolytic enzyme activities were measured by the dinitrosalicylic acid (DNS) method, which is related to polysaccharide disintegration (Miller, 1959). $MnSO_4$ and veratryl alcohol were used as substrates for measuring the oxidizing enzymes (manganese (II)-dependent peroxidase (MnP) and lignin peroxidase(LiP) (Glenn et al., 1986), and H_2O_2 was added to start the reaction, then the absorbance values were measured at 240 nm and 310 nm using a UV-5500PC spectrophotometer (Arora and Gill, 2001). Laccase activities were assayed spectrophotometrically with 2, 2-azino-bis-3-ethylthiazoline-6-sulfonate (ABTS) as substrate, and the change of absorbance value at 420 nm was recorded (Grassin and Dubourdieu, 1986).

2.4. Crystallinity, chemical characterization and morphological observation

The chemical characteristics of bamboo before and after fungal erosion were analyzed using Fourier transform infrared (FTIR) spectroscopy on an FTIR-650 spectrometer (Tianjin Gangdong Sci. & Tech. Development Co., Ltd.). Bamboo sieved powder before and after fungal erosion was mixed with KBr at a weight ratio of 1:100 before the spectrum collection. For each measurement, 32 scans were performed in the wave number region between 4000 cm^{-1} and 500 cm^{-1} with a resolution of 4 cm^{-1}.

The X-ray diffraction (XRD) analysis was performed using a Rigaku Ultima IV diffractometer (Rigaku Corporation, Japan) operating in continuous scanning mode to determine the crystallinity index of both control and pretreated samples. The XRD pattern was recorded every 0.020 (2θ) at the angle range of 5°–40° with the scanning speed of 8° min^{-1}. The acquired XRD patterns were processed using MDI Jade software to calculate the crystallinity index. After smoothing and background subtraction, each pattern was deconvoluted into crystalline and amorphous regions through peak fitting. The crystallinity was quantitatively determined by integrating the area under the crystalline peaks (Ac) and the total area (At, including both crystalline and amorphous contributions), followed by application of the formula: Crystallinity (%) = (Ac / At) × 100. All measurements were conducted in triplicate to ensure reliability and reproducibility.

Qualitative and semi-quantitative analysis of the surface elemental composition and chemical states of bamboo specimens was performed using a K-Alpha X-ray photoelectron spectrometer (Thermo Fisher Scientific, USA). Samples were sectioned into 5 mm × 5 mm flakes and mounted on a conductive sample stage. Measurements were conducted under ultra-high vacuum (< 2.0 × 10^{-7} mbar) using monochromated Al Kα radiation (hν = 1486.6 eV) with an operating voltage of 12 kV, filament current of 6 mA, and a spot size of 400 μm. The relative elemental concentrations were determined by normalizing characteristic peak areas using Thermo Avantage software.

To evaluate the chemical composition, the control and fungal pretreated bamboos were ground using a hammer mill to pass a 40–60 mesh screen. Chemical composition determination was carried out in accordance with the procedures of the National Renewable Energy Laboratory (NREL, Golden, CO, USA) standard. Glucose and xylose contents were measured by dinitrosalicylic acid (DNS) method.

The analysis of lignin structural changes was carried out by two-dimensional heteronuclear single quantum coherence (2D-HSQC) spectra, and two-dimensional nuclear magnetic resonance (2D NMR) spectra were acquired on a Bruker 500 MHz NMR spectrometer. 20 mg of bamboo powder was swollen in dimethyl sulfoxide-DMSO- d_6 (99.8 % D) for 2D NMR.

The content of phenolic hydroxyl groups was determined by colorimetric method. Phenolic compounds could reduce W^{6+} to W^{5+}, then produce blue complex under alkaline conditions, which has maximum absorption at 760 nm and the absorption value was positively correlated with the content of phenolic hydroxyl group.

For Morphological observation, a scanning electron microscope (SEM, Hitachi TM 3000, Japan) with an acceleration voltage of 15–20 KV was used to monitor the changes of microscopic structure and mycelial distribution.

2.5. Statistical analysis

The statistical analyses were performed using SPSS Statistics (Version 27.0; IBM Corp., Armonk, NY, USA). Measurement data are

presented as the mean ± standard deviation. The significance level was set at $\alpha = 0.05$, and p-values < 0.05 were considered statistically significant.

3. Results and discussion

3.1. Mass changes with biodeterioration of filamentous strains

The mass loss of *D. sinicus* samples in various stages is given in Table 1. *A. niger* caused significantly greater mass loss in *D. sinicus* than *P. citrinum* and *T. viride*, suggesting substantial structural compromise as the progressive degradation culminated in a mass loss exceeding 10 % after 90 days. Its accelerated kinetics (Δ2.15 %, 60–90 days) correlated with superior lignocellulolytic competence, likely through enhanced cellulase/xylanase secretion during prolonged colonization (Irbe et al., 2006; Liu et al., 2015). While *T. viride* showed intermediate degradation (6.21–8.49 %), and *P. citrinum* minimal impact (2.51–5.93 %). Consequently, *A. niger* emerged as the primary biodeterioration agent for *D. sinicus*, necessitating prioritized targeting in biocontrol strategies through inhibition of its hyphal proliferation and enzymatic activity to mitigate infrastructure degradation.

3.2. Extracellular enzymatic activities

Comparative profiling of lignocellulolytic enzyme activities was performed to elucidate enzymatic drivers underlying strain-specific biodeterioration patterns, testing whether superior degradation kinetics during bamboo colonization correlate with differential enzyme expression profiles (Fig. 2, Table S1-S3).

3.2.1. A. niger

A. niger employed a staged enzymatic synergy to degrade *D. sinicus* (Fig. 3, a-c). During initial colonization (10 days), explosive secretion of endoglucanase (65.45 mL^{-1}) and exoglucanase (107.88 mL^{-1}) rapidly dismantled cellulose frameworks, concurrently with peak activities of xylanase (75.05 mL^{-1}), amylase (64.23 mL^{-1}), and pectinase (156.65 mL^{-1}) targeting hemicellulose, starch granules, and pectin-rich middle lamellae (O'NEILL et al., 1990; Thompson, 2000). This coordinated assault primarily compromised non-lignified components. The mid-phase (10–60 days) sustained steady xylanase and pectinase production for continuous matrix deconstruction, while declining amylase activity indicated depletion of labile carbon sources. Crucially, by the late stage (80 days), MnP was specifically activated (peak 613.10 mL^{-1}), cleaving phenolic lignin subunits (β-*O*-4 linkages) via a single-electron oxidation mechanism. This generated phenoxy radicals that initiated polymer depolymerization, ultimately disrupting the exposed lignin barrier (Hatakka and Hammel, 2010; Mäkelä et al., 2002; Martin, 2002). This saccharification-first delignification strategy, characterized by the sequential prioritization of carbohydrate hydrolysis followed by lignin modification, enabled efficient deconstruction of bamboo's recalcitrant cellulose-lignin matrix through temporally optimized enzyme deployment.

3.2.2. P. citrinum

The degradation of *D. sinicus* by *P. citrinum* exhibited a characteristic "delignification-first saccharification-later" temporal pattern, yet was fundamentally constrained by critical enzymatic deficiencies (Fig. 3, d-f). During initial colonization (10 days), MnP activity peaked transiently (333.73 mL^{-1}) before rapidly decaying, resulting in incomplete lignin depolymerization that compromised subsequent degradation. As the process progressed to the critical phase (40–50 days), coordinated hydrolase activity emerged: endoglucanase (168.88 mL^{-1}) and exoglucanase (215.75 mL^{-1}) efficiently dismantled cellulose microfibrils, xylanase (194.06 mL^{-1}) persistently degraded hemicellulose networks, pectinase (218.6 mL^{-1}1) specifically targeted bamboo's characteristically pectin-rich middle lamella, while amylase (176.28 mL^{-1}) focused on starch granule hydrolysis. However, the premature termination of delignification created regenerated lignin barriers during peak hydrolase activity, severely limiting degradation efficacy. This spatiotemporal coordination deficit ultimately reduced overall degradation efficiency (5.93 %) significantly below *A. niger*'s performance (10.97 %), conclusively demonstrating that efficient bamboo degradation required not merely high enzyme activity, but precisely orchestrated temporal sequencing and spatial distribution of the entire enzymatic system.

Table 1
Mass losses of *D. sinicus* subjected to filamentous stains.

	Mass loss (%)		
Time (days)	30	60	90
A. niger	8.17	8.82	10.97
P. citrinum	2.51	4.05	5.93
T. viride	6.21	7.07	8.49

3.2.3. T. viride

The degradation of *D. sinicus* by *T. viride* exhibited a distinctive phased enzymatic synergy (Fig. 3, g-i). During mid-stage colonization (30 days), MnP (190.32 mL^{-1}) first peaked, with its moderate lignin depolymerization establishing the foundation for subsequent hydrolysis. Entering the critical degradation phase (40–60 days), the hydrolase system displayed precisely coordinated activation: endoglucanase (119.9 mL^{-1} at 60 days) and exoglucanase (178.23 mL^{-1} at 50 days) synergistically deconstructed cellulose microfibrils, xylanase (132.85 mL^{-1} at 50 days) targeted hemicellulose networks, amylase (181.54 mL^{-1} at 40 days) efficiently degraded bamboo starch granules, while pectinase (180.4 mL^{-1} at 50 days) continuously disrupted the middle lamella. This "tightly coupled lignin-hydrolase biphasic strategy" partially overcame the temporal defects observed in *P. citrinum*, enabling hydrolases to function effectively within the lignin modification window. However, the peak activity of its sole ligninolytic enzyme (190.32 mL^{-1}) was 67.5 % lower than *A. niger* (613.10 mL^{-1}), and the overall hydrolase activities were generally weaker than *P. citrinum*, resulting in insufficient deep-structure dissociation and ultimately yielding an intermediate degradation rate of 8.49 % at 90 days. These findings demonstrated that degradation efficiency was dually regulated by both enzymatic activity intensity and spatiotemporal coordination.

The biological degradation of bamboo fundamentally represented a spatiotemporally regulated process mediated through fungal enzymatic synergy, where the optimized overlap between the lignin-depolymerizing window and hydrolase-sustaining phase constituted a critical threshold for degradation efficacy. This theoretical framework not only elucidates the molecular essence of bamboo biodeterioration but also establishes a novel paradigm for developing temporally targeted preservation technologies through precise modulation of key enzymatic activity windows, thereby significantly enhancing the biological durability of bamboo products and demonstrating substantial engineering significance for advancing sustainable bamboo resource utilization.

3.3. Analysis of chemical components in supernatants

The chemical components in supernatants were analyzed to further understand their relationships with extracellular enzyme activities throughout the *D. sinicus* biodeterioration process (Fig. 3 and S1, Table S4). The enzymatic degradation of bamboo components exhibited distinct substrate-specific mechanisms. Cellulase systems (endoglucanase and exoglucanase) demonstrated a strong positive correlation between activity peaks and glucose concentration in supernatants, reflecting their cascade catalytic mechanism: endoglucanases randomly cleaved β-1,4-glycosidic bonds in cellulose chains to generate new reducing ends, while exoglucanases progressively released cellobiose from these termini, subsequently hydrolyzed to glucose by β-glucosidase, establishing a linear "enzyme activity-product accumulation"

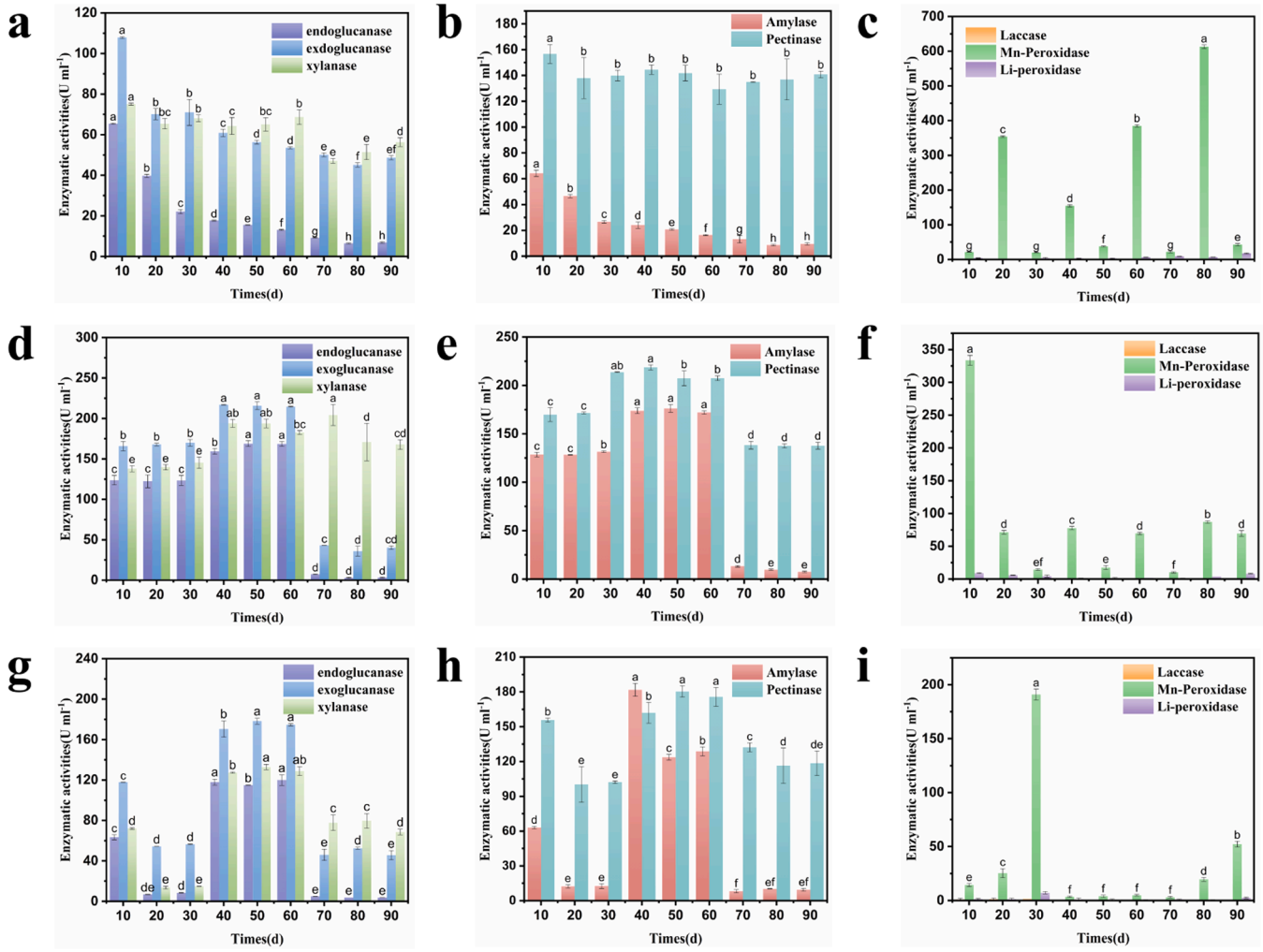

Fig. 2. Lignocellulolytic enzymes activities during the biodeterioration of *D. sinicus* by a-c: *A. niger*; d-f: *P. citrinum*; g-i: *T. viride*. Different lowercase letters above the bars indicate significant differences among groups according to Tukey's test ($p < 0.05$).

response (Li et al., 2022). Similarly, hemicellulases (particularly xylanase) showed synchronized action with xylan degradation, where xylanase specifically hydrolyzed α-1,4 linkages between xylose units to directly yield xylo-oligosaccharide monomers (Zhang et al., 2017a). In contrast, lignin content demonstrated weaker correlation with MnP activity due to the indirect and complex nature of lignin depolymerization: MnP generated phenoxyl radicals via single-electron oxidation that initiated non-enzymatic chain reactions, with degradation efficiency constrained by spatial hindrance from lignin-carbohydrate complexes (LCCs) and radical recombination, resulting in delayed substrate conversion relative to enzymatic activity peaks (Tan et al., 2022; Wang et al., 2025).

3.4. Chemical composition and structural analysis

The fungal degradation of *D. sinicus* exhibited strain-specific temporal strategies (Fig. 4a-c, Table S5). Universally, hemicellulose was prioritized, with xylose content decreased from 25.69 % to 12–15 % within 30 days, originating from the accessibility of hemicellulose's amorphous structure and efficient α-1,4-bond hydrolysis by xylanases (Danrui et al., 2015). Strain-specific patterns emerged: *A. niger* employed an inside-out cellulose-priority strategy, where early cellulase burst (30 days) reduced glucose from 40.30 % to 38.40 %, while delayed MnP effectively oxidized exposed lignin only in the final stage (90 days, 30.58–28.68 %). *P. citrinum* executed a surface-first lignin-priority approach, with initial MnP rapidly degrading surface lignin (31.72–27.88 % at 30 days), but enzymatic replenishment failure caused barrier regeneration (rebound to 28.66 % at 90 days). *T. viride* achieved synchronous deconstruction via coordinated cellulase and MnP at 30 days, concurrently reducing glucose (40.30–31.83 %) and lignin (31.72–26.24 %). Its lower MnP activity yielded superior lignin degradation, confirming radical chain reactions' dominance (Ali et al., 2020). This temporal differentiation provided precise targets for bamboo preservation, specifically enhancing bamboo durability by blocking *A. niger*'s cellulase system, inhibiting initial MnP activation in *P. citrinum*, and quenching free radical chains in T. *viride*.

Based on the FTIR spectral characteristics (Fig. 4d-f), the fungal (*A. niger*, *P. citrinum*, and *T. viride*) degradation of *D. sinicus* exhibited a sharp attenuation in the hemicellulose carbonyl peak (1735 cm^{-1}) (Li et al., 2010), which was directly attributed to the targeted hydrolysis of abundantly exposed acetyl ester bonds within its amorphous structure by fungal-secreted xylanases (Zhang et al., 2017b), enabling rapid acquisition of readily metabolizable carbon sources such as xylose. Concurrently, the progressive weakening of lignin characteristic peaks (phenolic C–O at 1245 cm^{-1} and aromatic C=C at 1500–1600 cm^{-1}) correlated with MnP-driven oxidation mechanisms, wherein MnP oxidized Mn^{2+} to Mn^{3+}, subsequently attacking ether linkages and aromatic rings in phenolic lignin subunits (Xu et al., 2013; Yan et al., 2016). In contrast, the stability of the cellulose skeletal peak (C–O at 1025 cm^{-1}) was attributed to the physical barrier formed by dense

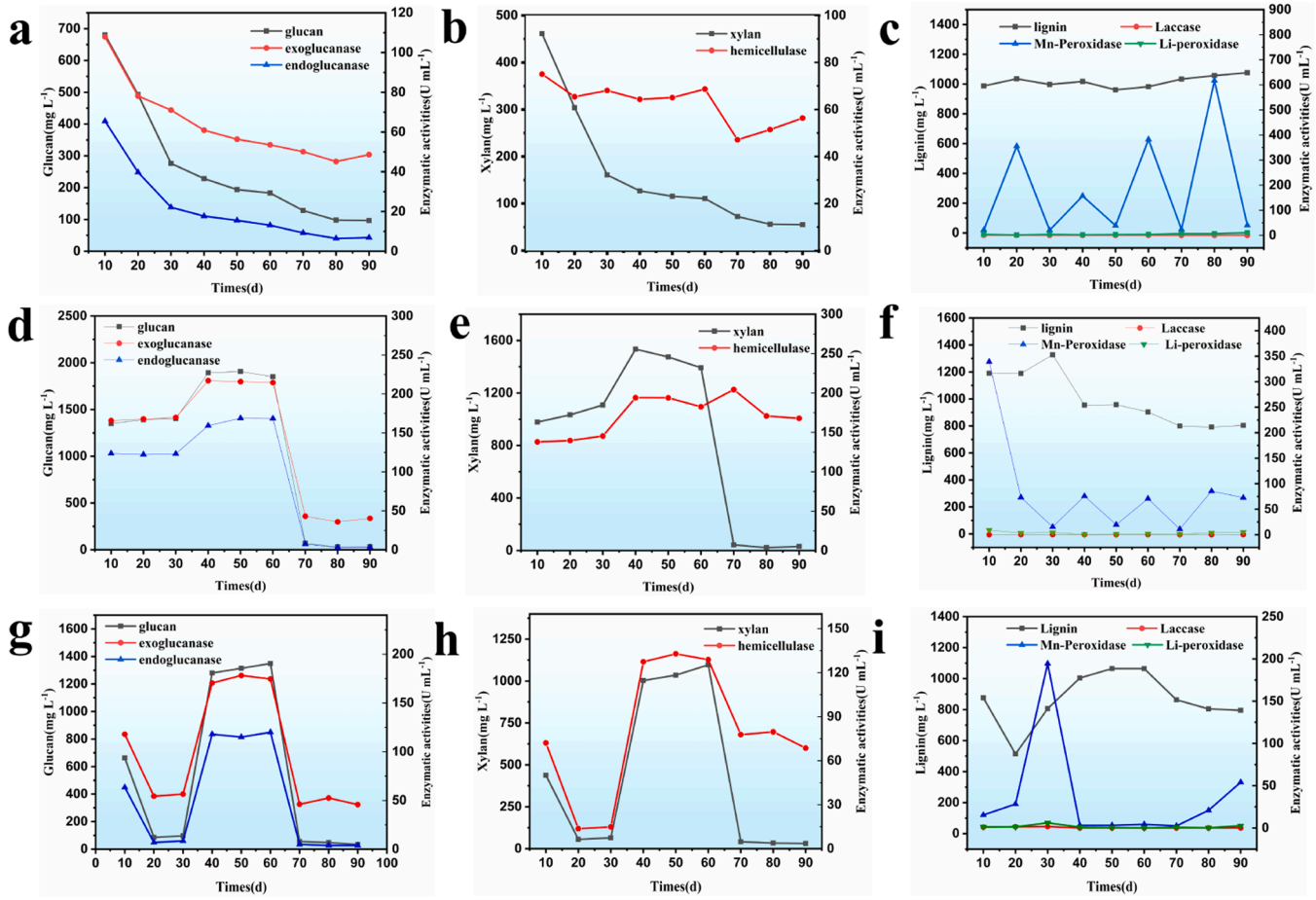

Fig. 3. The relationships between chemical compositions and enzyme activities in supernatants during enzymatic biodeterioration process. a-c: *A. niger*; d-f: *P. citrinum*; g-i: *T. viride*.

hydrogen-bonding networks in crystalline regions, which remained resistant to enzymatic deconstruction under the fungal energy-optimization strategy favoring preferential utilization of labile components (Asada et al., 2021; Yang et al., 2021). This hierarchical degradation mechanism essentially represented an adaptive evolutionary strategy wherein fungi balanced energy efficiency (prioritizing low-resistance hemicellulose) with substrate accessibility (sequentially dismantling LCC barriers) (Marcolongo et al., 2014; Wang et al., 2013).

The crystallinity changes of *D. sinicus* during degradation by three fungal species exhibited significant variations, primarily determined by the temporal coordination between lignin degradation and cellulase attack (Fig. 4g-i, Table S6). For *A. niger*, although early peaks of cellulase and xylanase activities were observed at 10 days, the significantly delayed peak of ligninolytic MnP activity at 80 days resulted in persistent lignin barriers. This severely limited the efficiency of cellulase attack on crystalline regions, ultimately leading to minimal crystallinity reduction (merely 3.83 %) after 90 days. *P. citrinum* demonstrated a distinct degradation pattern. Its early peaks of MnP activity (10 days) and xylanase activity (40 days) facilitated preferential degradation of lignin (12.1 %) and hemicellulose (45 %) by 30 days. However, the delayed peak of cellulase activity at 50 days resulted in insufficient attack on crystalline regions, yielding a moderate crystallinity reduction of 5.25 % at 90 days. *T. viride* exhibited the highest degradation efficiency due to synchronized peaks of MnP (30 days) and cellulase (50 days) activities. This coordination enabled concurrent degradation of lignin (17.3 %) and cellulose (21.0 %) by 30 days, leading to a remarkable 28 % crystallinity reduction at 60 days. These results clearly demonstrated that crystallinity changes depended not only on the absolute enzymatic activities, but more crucially on the temporal matching of enzymatic activity peaks and their synergistic effectiveness in overcoming lignin barriers and attacking cellulose crystalline regions (Larran et al., 2015).

XPS analysis of *D. sinicus* following 90-day fungal erosion revealed shared and species-specific degradation mechanisms (Fig. 5, Table S7-8). All molds mediated silica dissolution via secreted organic acids, reducing silicon content from 1.79 % to 0.77–1.25 %, which relatively enriched organic carbon (C% increased from 65.39 % to 65.67–66.30 %). Differential oxygen-nitrogen dynamics and carbon speciation indicated distinct degradation pathways. Following *A. niger* infestation, the oxygen content increased by 1.13 % (from 29.96 % to 31.09 %) with the C-O-C bond proportion rising to 12.16 %, attributed to its preferential degradation of hemicellulose releasing oligosaccharide fragments, coupled with cellulose oxidation generating carbonyl groups (C═O bonds increased to 57.88 %). *P. citrinum* reduced oxygen content by 1.00 % (to 28.96 %) and maintained stable C-C/C-H bonds through preferential degradation of lignin aromatic rings (low-oxygen C-C structures), which enriched carbon skeletons. Simultaneously, it caused a 13.8 % nitrogen increase (2.72 % vs. 2.39 %) by secreting nitrogenous biofilms. Conversely, *T. viride* exhibited synergistic hydrolysis-oxidation, where glycosidic bond cleavage (C–O–C decreased sharply to 6.76 %) coupled with intense oxidation (C═O surged to 64.93 %) compromised the carbon skeleton (C–C reduced to 28.31 %), ultimately driving net nitrogen loss (N declined to 2.05 %) and oxygen dynamic equilibrium (O stabilized at 29.87 %).

3.5. 2D-HSQC NMR analysis

To further investigate the typical structural features of lignin

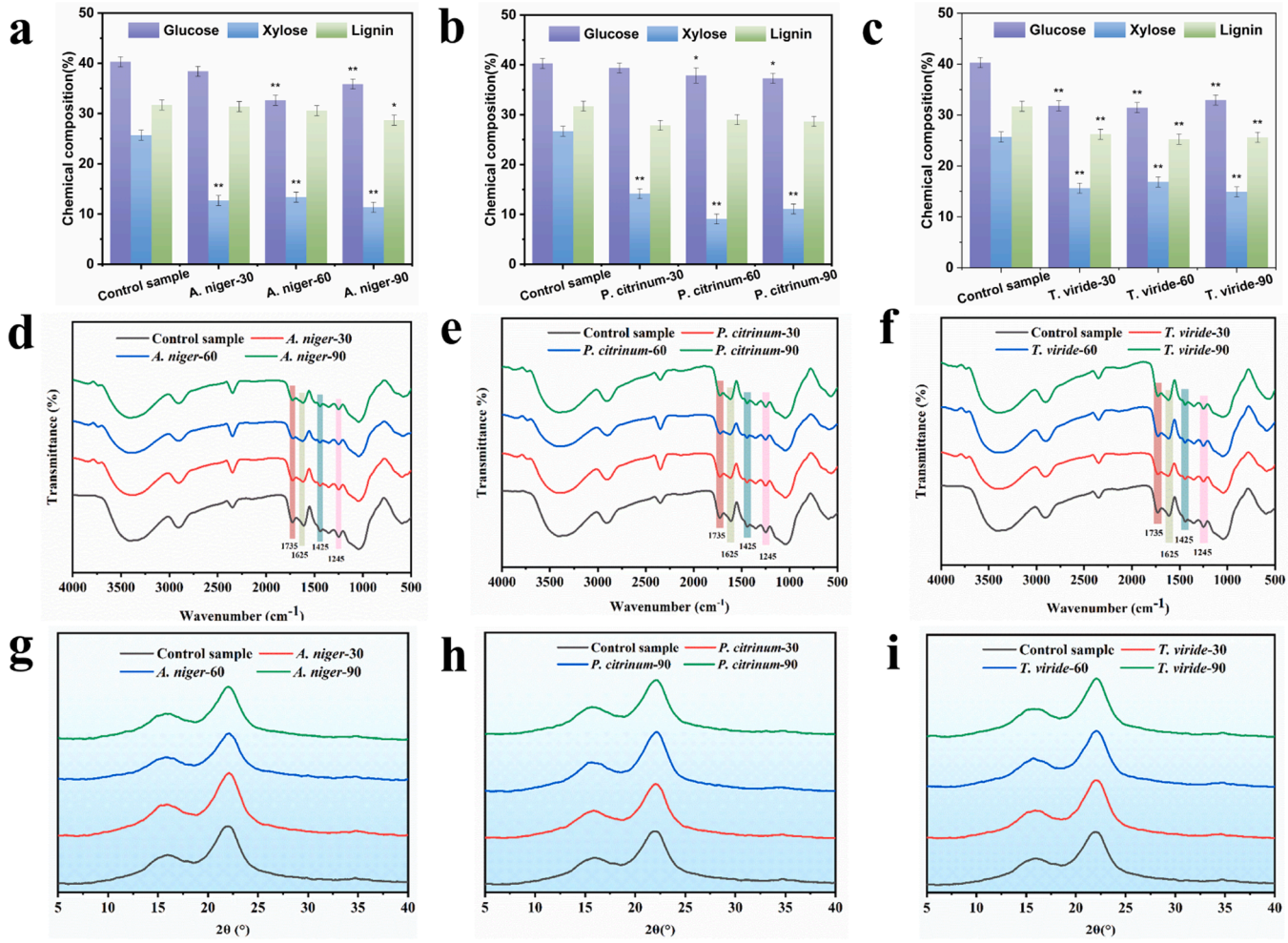

Fig. 4. The changes in chemical composition and structure of *D. sinicus* samples during biodeterioration process. Asterisks (*) and (**) indicate significant difference, ($p < 0.05$) and ($p < 0.01$), respectively, compared with the control group by Wilcoxon signed rank test.

obtained after filamentous stain process, double enzymatic lignin (DEL) samples were characterized by the 2D-HSQC investigation (Fig. 6). The side-chain and aromatic regions in 2D-HSQC NMR spectra and the substructures were assigned, referring to previous publications (Wen et al., 2013a). It could be observed that the DELs from *D. sinicus* were a typical *gramineous* lignin (Shi et al., 2013). The substructures, such as β-O-4 aryl ethers (A), resinol (B, β-β), phenylcoumaran (C, β-5) and p-hydroxycinnamyl alcohol end group (I) were detected in the side-chain regions. In the aromatic region, signals from syringyl (S), guaiacyl (G), p-hydroxyphenyl (H), *p*-counmarate ester (PCE), trincin substructures (T) and ferulate ester substructures (FA) were well distinguished.

The quantification of characteristic correlated signals was adopted to analyze the changes of chemical composition and relative content of different linkages (Kim and Ralph, 2010; Wen et al., 2013b), and the result is given in Fig. 6. The selective degradation of β-β/β-5 condensed linkages by *A. niger* led to the disruption of lignin's rigid framework, while *P. citrinum* and *T. viride* primarily cleaved β-*O*-4 ether bonds, resulting in polymer backbone depolymerization. All three fungal groups caused a decrease in *p*-coumarate ester (PCE) content, indicating ester bonds as common degradation targets. The reduced S/G ratio observed after *A. niger* and *P. citrinum* infestation confirmed the preferential degradation of syringyl (S) units (Yan et al., 2016). These findings were further supported by hydroxyl content variations (Table S9): *A. niger* infestation induced a 44.7 % surge in hydroxyl groups (2.6266 vs 1.8154 mmol g^{-1}) due to β-β/β-5 bond cleavage, whereas *P. citrinum* and *T. viride* groups showed smaller hydroxyl increases (5.0–11.4 %) corresponding to exclusive β-*O*-4 bond scission. Consequently, bamboo protection required the development of cross-linking preservatives specifically stabilizing β-β/β-5 condensed structures against *A. niger*'s characteristic degradation, along with phenolic antioxidants protecting β-*O*-4 ether linkages, providing crucial theoretical foundations for precision mold-proof technologies based on lignin structural characteristics (Yelle et al., 2008).

3.6. Morphology observation

The microstructural degradation of *D. sinicus* induced by three mold species progressed through three sequential phases (Fig 7, S2). Initially, mold spores colonized the intercellular spaces where highly active amylases and pectinases rapidly degraded starch granules and pectins to generate nutrients for fungal proliferation, resulting in accumulated hyphae and secretions within these spaces although the cell walls remained largely intact despite potential weakening of intercellular bonding due to pectin decomposition. As colonization advanced, cellulases, hemicellulases and MnP became predominant and progressively degraded the cell wall structural components, leading to significantly increased porosity. This multi-stage synergistic deterioration pattern, transitioning from consumption of readily decomposable nutrients (starch, pectin) for colonization to ultimate disintegration of structural materials, culminated in catastrophic loss of mechanical integrity. Consequently, targeted bamboo preservation required a tripartite

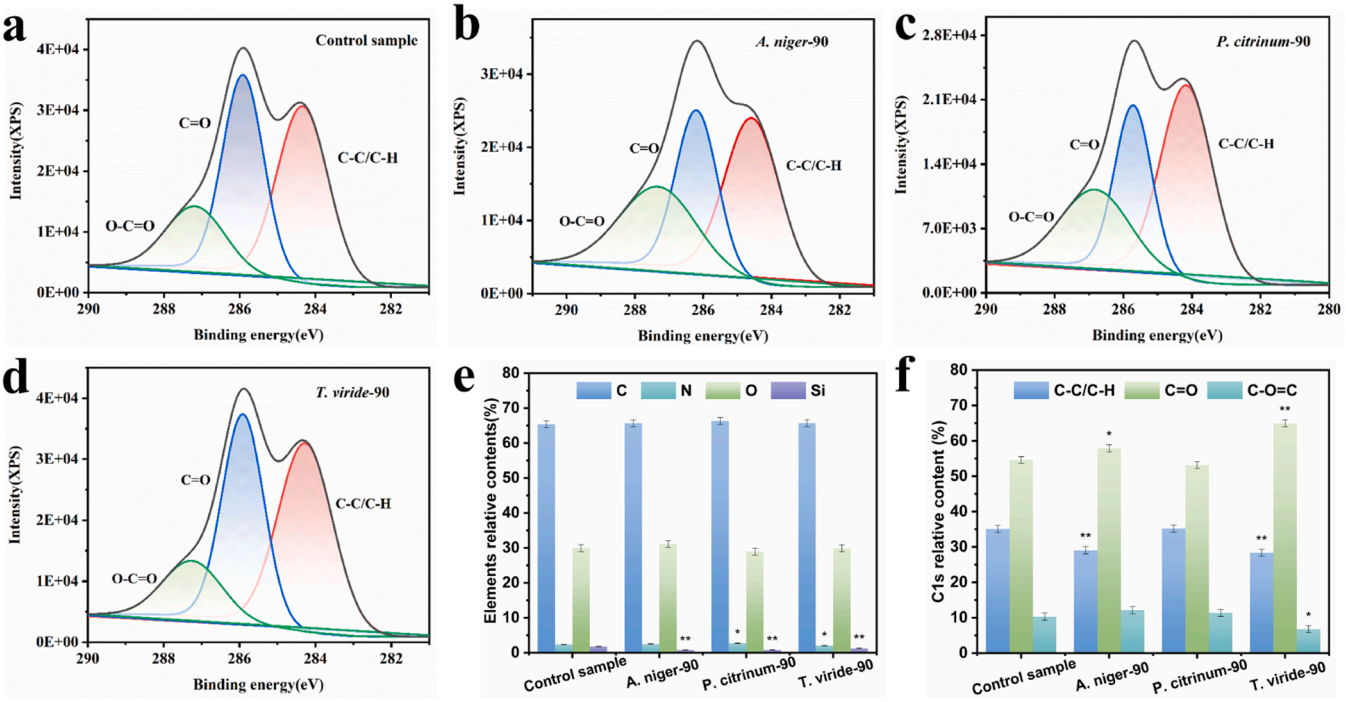

Fig. 5. XPS analysis of *D. sinicus* samples during biodeterioration process. Asterisks (*) and (**) indicate significant difference, ($p < 0.05$) and ($p < 0.01$), respectively, compared with the control group by the Wilcoxon signed rank test.

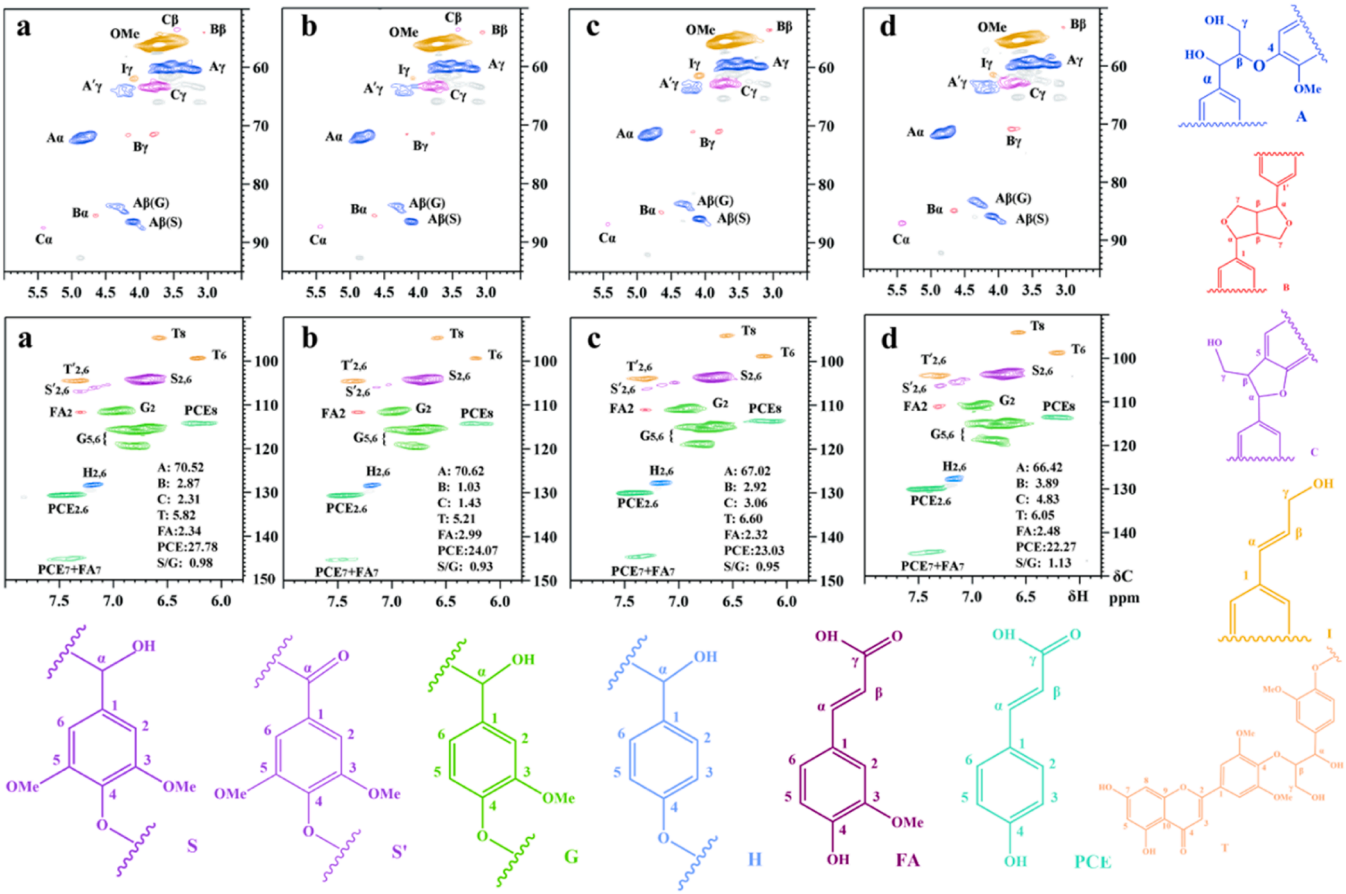

Fig. 6. Side-chain and aromatic regions in the 2D-HSQC NMR spectra, quantification of lignin fractions and the main identified substructures of the DELs. a: Control sample; b: *A. niger*; c: *P. citrinum*; d: *T. viride*.

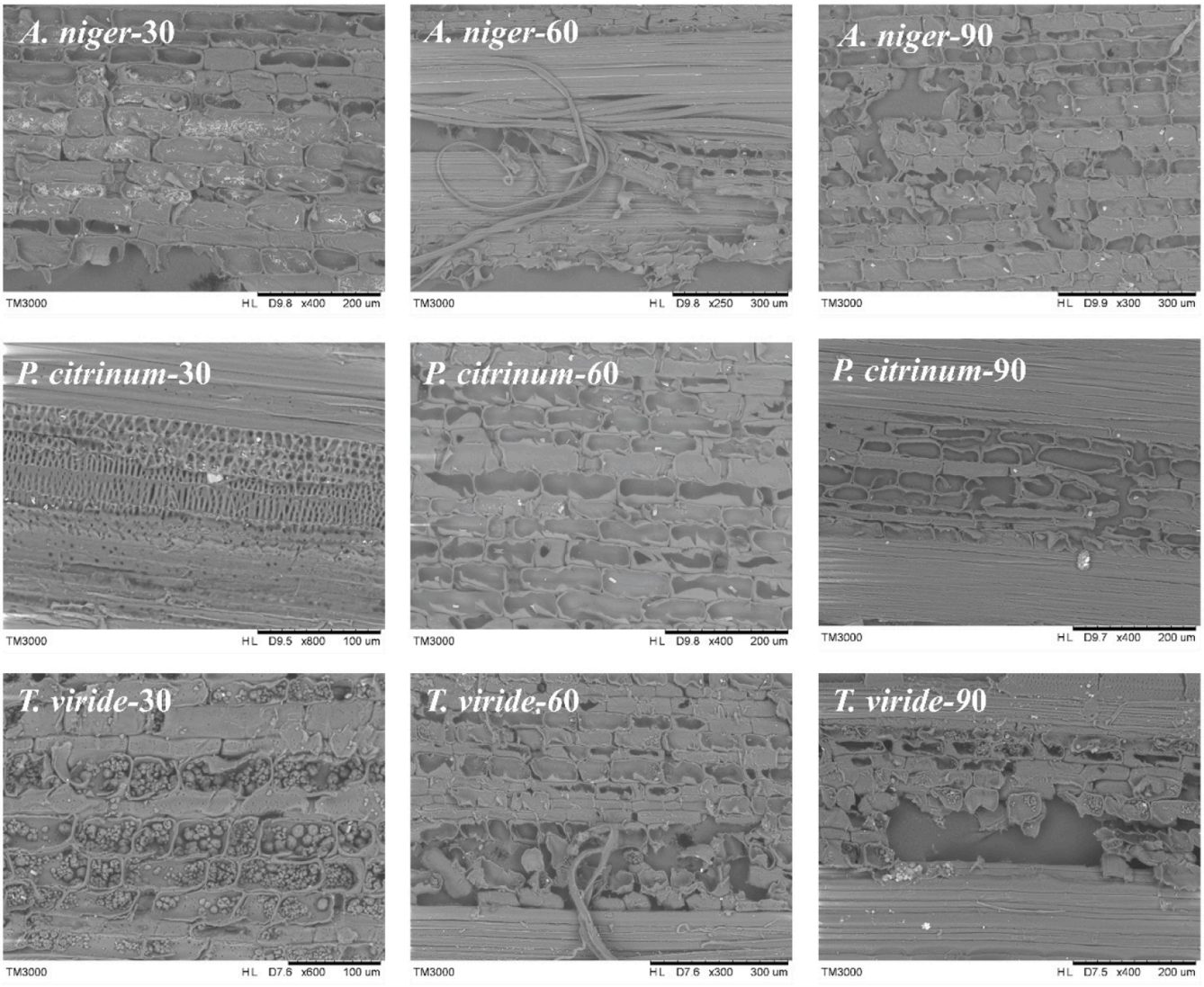

Fig. 7. SEM images of *D. sinicus* samples during biodeterioration process.

strategy initially involving pretreatment to degrade starch and pectin for eliminating colonization substrates followed by infusion of zinc borate-based crosslinking agents to reinforce cell walls through micro-pore filling and enzyme pathway inhibition and ultimately applying photocatalytic nanocoatings to establish dual physical-chemical spore barriers thereby establishing a systemic anti-mold defense mechanism (Mai et al., 2022; Prosper et al., 2018; Zhou et al., 2023).

In summary, *A. niger*, *P. citrinum*, and *T. viride* exhibited distinct species-specific degradation patterns when colonizing *D. sinicus*. This observation aligned with the fundamental principles of lignocellulose degradation, wherein microbial degradation efficiency was governed by both substrate composition and species-specific enzymatic strategies (Zhao et al., 2025). Specifically, substrate composition influenced the degradation process through the spatial architecture and chemical barriers of lignin-carbohydrate complexes, while different fungal species employed unique enzyme secretion profiles and metabolic pathways to implement differentiated degradation behaviors (Zhang et al., 2017a; Zhao et al., 2021). Furthermore, *D. sinicus*, due to its distinctive physical structure and chemical composition, induced microbial responses that differed markedly from those observed in conventional wood or straw substrates, underscoring its uniqueness as a lignocellulosic material (Chen et al., 2025b; Wang et al., 2022). Based on these findings, this study proposes a theoretical foundation for a "precision preservation" strategy. This approach advocates moving beyond broad-spectrum antimicrobial methods toward targeted interventions against specific infestation pathways employed by different fungal species in *D. sinicus*. Such interventions include, but are not limited to, impeding the attack on internal cellulose by *A. niger* and disrupting the synergistic degradation at the lignin-cellulose interface by *T. viride*. Ultimately, this enables the establishment of a tailored protection system based on specific fungus-substrate interactions.

4. Conclusions

This study systematically elucidated the species-specific degradation mechanisms of *D. sinicus* by three primary molds including *A. niger*, *P. citrinum*, and *T. viride*. The results demonstrated that the core efficiency of mold degradation in *D. sinicus* relied on the spatiotemporal overlap between the lignin decomposition window and the hydrolase activity period. While hemicellulose served as the primary and preferentially attacked component for all three mold species, they employed divergent strategies for decomposing the bamboo structure. Specifically, *A. niger* employed an inward-to-outward cellulose-prioritized pathway, *P. citrinum* executed a surface-oriented lignin-prioritized strategy, and *T. viride* simultaneously degraded both cellulose and lignin components. Lignin structural analysis confirmed that *A. niger* selectively attacked β-β

and β-5 condensed linkages to disrupt the rigid framework, whereas *P. citrinum* and *T. viride* primarily cleaved β-*O*-4 ether bonds to achieve backbone depolymerization, with all three species consistently targeting ester bonds. Microstructural evolution clearly demonstrated a continuous three-stage degradation pattern comprising initial colonization consuming readily decomposable substances, followed by enzyme-driven cell wall deconstruction causing a sharp increase in porosity, and culminating in structural collapse. Collectively, these findings decode the specialized enzymatic and mechanistic bases of mold-induced biodeterioration in *D. sinicus*. The clarified species-specific strategies provide a fundamental theoretical foundation for understanding fungal pathogenesis in lignocellulosic biomass and establish a crucial knowledge platform for future development of targeted preservation technologies.

CRediT authorship contribution statement

Mizi Fan: Writing – review & editing, Visualization, Conceptualization. **Yonghui Zhou:** Writing – review & editing, Conceptualization. **Jiyun Qi:** Writing – review & editing, Visualization, Methodology, Investigation, Formal analysis. **Yan Xia:** Writing – review & editing, Visualization, Data curation, Conceptualization. **Chen Zhang:** Methodology. **Jialong Wen:** Writing – review & editing, Methodology, Conceptualization.

Declaration of Competing interest

The authors declare that they have no known competing financial interests or personal relationships that could have appeared to influence the work reported in this paper.

Acknowledgments

The authors are grateful for the financial support from the Regional Project of the National Natural Science Foundation of China (32260362), the Joint project of Yunnan Agricultural Basic Research (202401BD070001–025), the Foreign Experts Project of Yunnan Province (202505AO120007), the Reserve Talent Project for Young and Middle-aged Academic and Technical Leaders of Yunnan Province (202405AC350033), and the 111 Project (D21027).

Appendix A. Supporting information

Supplementary data associated with this article can be found in the online version at doi:10.1016/j.indcrop.2025.122394.

Data availability

The authors do not have permission to share data.

References

Ali, N., Giwa, A.S., Abdalla, M., Liu, X., 2020. Alkaline hydrogen peroxide pretreatment of bamboo culm for improved enzymatic release of reducing sugars using recombinant cellulases. Cellulose 27, 769–779. https://doi.org/10.1007/s10570-019-02829-8.

Arora, D.S., Gill, P.K., 2001. Comparison of two assay procedures for lignin peroxidase. Enzym. Micro Tech. 28, 602–605. https://doi.org/10.1016/s0141-0229(01)00302-7.

Asada, C., Yoshida, Y., Nakamura, Y., 2021. Efficient conversion of moso bamboo components into glucose, lignocellulose nanofiber, and low-molecular-weight lignin through deep eutectic solvent treatment. Biomass.. Convers. Biorefinery 1–12. https://doi.org/10.1007/s13399-021-01629-0.

Bao, Q., Yang, F., Zhang, S., Zhu, J., Du, C., Ran, Y., Tao, P., Ding, J., Wang, X., Yin, W., 2025. Selective impact of lignin and hemicelluloses macromolecules in bamboo cell walls by mildew. Int. J. Biol. Macromol. 306, 141495. https://doi.org/10.1016/j.ijbiomac.2025.141495.

Chen, Y., Deng, L., Han, W., Wang, J., Wang, E., Liang, Y., Miao, Y., Hu, L., Huang, J., 2025b. Construction of lignin-derived microcapsule anti-mildew system with excellent anti-loss performance for Masson pine wood protection. Int J. Biol. Macromol. 294, 140059. https://doi.org/10.1016/j.ijbiomac.2025.140059.

Chen, S., Lv, Y., Chen, C., Xu, J., Xiao, Y., Ge, J., 2025a. Risk assessment of mold growth on engineered bamboo and its application. Build. Environ. 267, 112306. https://doi.org/10.1016/j.buildenv.2024.112306.

Danrui, C., Zhengjun, S., Haiyan, Y., Zhengdiao, M., Weiyi, L., Zhifeng, Z., Chaomao, H., jia, D., 2015. Chemical structure of lignin isolated from *Dendrocalamus sinicus*. Word Bamboo Ratt. 13, 1–6. https://doi.org/10.13640/j.cnki.wbr.2015.02.001.

Glenn, J.K., Akileswaran, L., Gold, M.H., 1986. Mn (II) oxidation is the principal function of the extracellular Mn-peroxidase from Phanerochaete chrysosporium. Arch. Biochem Biophys. 251, 688–696. https://doi.org/10.1016/0003-9861(86)90378-4.

Grassin, C., Dubourdieu, D., 1986. Optimisation de la méthode de dosage de l'activité laccase de Botrytis cinerea par la syringaldazine. Oeno One 20, 125–130. https://doi.org/10.20870/oeno-one.1986.20.2.1298.

Hatakka, A., Hammel, K.E., 2010. Fungal biodegradation of lignocelluloses. Ind. Appl. 319–340. https://doi.org/10.1007/978-3-642-11458-8_15.

Irbe, I., Andersons, B., Chirkova, J., Kallavus, U., Andersone, I., Faix, O., 2006. On the changes of pinewood (Pinus sylvestris L.) chemical composition and ultrastructure during the attack by brown-rot fungi Postia placenta and Coniophora puteana. Int. Biodeterior. Biodegrad. 57, 99–106. https://doi.org/10.1016/j.ibiod.2005.12.002.

Jiankun, L., Zhexing, L., Quan, L., Jun, S., Shangxing, C., Lifen, L., Zhigang, W., 2019. Study on Main Chemical Composition and Dilute Acid Hydrolysis of *Phyllostachys edulis cv. pachyloen*. J. Southwest For. Univ. 39, 161–165. https://doi.org/10.11929/j.swfu.201901027.

Kim, H., Ralph, J., 2010. Solution-state ^{2}D NMR of ball-milled plant cell wall gels in DMSO-d6/pyridine-d5. Org. Biomol. Chem. 8, 576–591. https://doi.org/10.1039/b916070a.

Larran, A., Jozami, E., Vicario, L., Feldman, S.R., Podesta, F.E., Permingeat, H.R., 2015. Evaluation of biological pretreatments to increase the efficiency of the saccharification process using Spartina argentinensis as a biomass resource. Bioresour. Technol. 194, 320–325. https://doi.org/10.1016/j.biortech.2015.06.150.

Lee, A.W., Chen, G., Tainter, F.H., 2001. Comparative treatability of Moso bamboo and Southern pine with CCA preservative using a commercial schedule. Bioresour. Technol. 77, 87–88. https://doi.org/10.1016/s0960-8524(00)00145-0.

Li, G.-y, Huang, A.-m, Qin, T.-f, Huang, L.-h, 2010. FTIR studies of masson pine wood decayed by brown-rot fungi. Spectrosc. Spectr. Anal. 30, 2133–2136. https://doi.org/10.3964/j.issn.1000-0593(2010)08-2133-04.

Li, N., Meng, F., Yang, H., Shi, Z., Zhao, P., Yang, J., 2022. Enhancing enzymatic digestibility of bamboo residues using a three-constituent deep eutectic solvent pretreatment. Bioresour. Technol. 346, 126639. https://doi.org/10.1016/j.biortech.2021.126639.

Liu, J., Sidhu, S.S., Wang, M.L., Tonnis, B., Habteselassie, M., Mao, J., Huang, Q., 2015. Evaluation of various fungal pretreatment of switchgrass for enhanced saccharification and simultaneous enzyme production. J. Clean. Prod. 104, 480–488. https://doi.org/10.1016/j.jclepro.2015.04.094.

Ma Xingxia, J.M., Qin, Daochun, 2012. Macro- and micro-structural changes in bamboo after attack by various fungi. Sci. Silvae Sin. 48, 76–82. https://doi.org/10.11707/j.1001-7488.20121112.

Mai, X., Mai, J., Liu, H., Liu, Z., Wang, R., Wang, N., Li, X., Zhong, J., Deng, Q., Zhang, H., 2022. Advanced bamboo composite materials with high-efficiency and long-term anti-microbial fouling performance. Adv. Compos Hybrid. Ma 5, 864–871. https://doi.org/10.1007/s42114-021-00380-4.

Mäkelä, M., Galkin, S., Hatakka, A., Lundell, T., 2002. Production of organic acids and oxalate decarboxylase in lignin-degrading white rot fungi. Enzym. Microb. Technol. 30, 542–549. https://doi.org/10.1016/S0141-0229(02)00012-1.

Marcolongo, L., Ionata, E., La Cara, F., Amore, A., Giacobbe, S., Pepe, O., Faraco, V., 2014. The effect of Pleurotus ostreatus arabinofuranosidase and its evolved variant in lignocellulosic biomasses conversion. Fungal Genet. Biol. 72, 162–167. https://doi.org/10.1016/j.fgb.2014.07.003.

Martin, H., 2002. Review: lignin conversion by manganese peroxidase (MnP). Enzym. Microb. Technol. 30, 454–466. https://doi.org/10.1016/S0141-0229(01)00528-2.

Miller, G.L., 1959. Use of dinitrosalicylic acid reagent for determination of reducing sugar. Anal. Chem. 31, 426–428. https://doi.org/10.1021/ac60147a030.

O'Neill, M., Albersheim, P., Darvill, A., 1990. The pectic polysaccharides of primary cell walls. Methods in plant biochemistry. Elsevier, pp. 415–441.

Prosper, N.K., Zhang, S., Wu, H., Yang, S., Li, S., Sun, F., Goodell, B., 2018. Enzymatic biocatalysis of bamboo chemical constituents to impart antimold properties. Wood Sci. Technol. 52, 619–635. https://doi.org/10.1007/s00226-018-0987-0.

Qi, J., Jia, L., Liang, Y., Luo, B., Zhao, R., Zhang, C., Wen, J., Zhou, Y., Fan, M., Xia, Y., 2022. Fungi's selectivity in the biodegradation of Dendrocalamus sinicus decayed by white and brown rot fungi. Ind. Crops Prod. 188, 115726. https://doi.org/10.1016/j.indcrop.2022.115726.

Saldarriaga-Hernández, S., Velasco-Ayala, C., Flores, P.L.-I., de Jesús Rostro-Alanis, M., Parra-Saldivar, R., Iqbal, H.M., Carrillo-Nieves, D., 2020. Biotransformation of lignocellulosic biomass into industrially relevant products with the aid of fungi-derived lignocellulolytic enzymes. Int. J. Biol. Macromol. 161, 1099–1116.

Shi, Z.-J., Xiao, L.-P., Deng, J., Sun, R.-C., 2013. Isolation and structural characterization of lignin polymer from *Dendrocalamus sinicus*. BioEnergy Res. 6, 1212–1222. https://doi.org/10.1007/s12155-013-9321-8.

Singh, S.K., 2021. Biological treatment of plant biomass and factors affecting bioactivity. J. Clean. Prod. 279, 123546. https://doi.org/10.1016/j.jclepro.2020.123546.

Sun, F., Zhou, Y., Bao, B., Chen, A., 2011. Influence of solvent treatment on mould resistance of bamboo. BioResources 6, 2091–2100. https://doi.org/10.5552/drind.2011.1106.

Tan, F., Cheng, J., Zhang, Y., Jiang, X., Liu, Y., 2022. Genomics analysis and degradation characteristics of lignin by Streptomyces thermocarboxydus strain DF3-3. Biotechnol. Biof Biop 15, 78. https://doi.org/10.1186/s13068-022-02175-1.

Thompson, D., 2000. On the non-random nature of amylopectin branching. Carbohydr. Polym. 43, 223–239. https://doi.org/10.1016/S0144-8617(00)00150-8.

Wang, L., Guan, H., Hu, J., Feng, Y., Li, X., Yusef, K.K., Gao, H., Tian, D., 2022. Aspergillus niger enhances organic and inorganic phosphorus release from wheat straw by secretion of degrading enzymes and oxalic acid. J. Agric. Food Chem. 70, 10738–10746. https://doi.org/10.1021/acs.jafc.2c03063.

Wang, Y., Wang, C., Ma, Z., Qin, L., Xu, L., Zhao, P., Li, K., 2025. Enzymatic degradation of lignin for valorization: A sustainable bridge towards advanced lignin-based biorefineries. Biomass.. Bioenerg. 202, 108231. https://doi.org/10.1016/j.biombioe.2025.108231.

Wang, W., Yuan, T., Cui, B., Dai, Y., 2013. Investigating lignin and hemicellulose in white rot fungus-pretreated wood that affect enzymatic hydrolysis. Bioresour. Technol. 134, 381–385. https://doi.org/10.1016/j.biortech.2013.02.042.

Wen, J.-L., Sun, S.-L., Xue, B.-L., Sun, R.-C., 2013a. Recent advances in characterization of lignin polymer by solution-state nuclear magnetic resonance (NMR) methodology. Materials 6, 359–391. https://doi.org/10.3390/ma6010359.

Wen, J.-L., Xue, B.-L., Xu, F., Sun, R.-C., Pinkert, A., 2013b. Unmasking the structural features and property of lignin from bamboo. Ind. Crops Prod. 42, 332–343. https://doi.org/10.1016/j.indcrop.2012.05.041.

Xiao, X., Liang, X., Peng, H., Wang, K., Liu, X., Li, Y., 2022. Multi-scale evaluation of the effect of thermal modification on chemical components, dimensional stability, and anti-mildew properties of moso bamboo. Polymers 14, 4677. https://doi.org/10.3390/polym14214677.

Xu, G., Shi, Z., Zhao, Y., Deng, J., Dong, M., Liu, C., Murugadoss, V., Mai, X., Guo, Z., 2019. Structural characterization of lignin and its carbohydrate complexes isolated from bamboo (Dendrocalamus sinicus). Int. J. Biol. Macromol. 126, 376–384.

Xu, G., Wang, L., Liu, J., Wu, J., 2013. FTIR and XPS analysis of the changes in bamboo chemical structure decayed by white-rot and brown-rot fungi. Appl. Surf. Sci. 280, 799–805. https://doi.org/10.1016/j.apsusc.2013.05.065.

Yan, K., Liu, F., Chen, Q., Ke, M., Huang, X., Hu, W., Zhou, B., Zhang, X., Yu, H., 2016. Pyrolysis characteristics and kinetics of lignin derived from enzymatic hydrolysis residue of bamboo pretreated with white-rot fungus. Biotechnol. Biofuels 9, 1–11. https://doi.org/10.1186/s13068-016-0489-y.

Yang, J., Xu, H., Jiang, J., Zhang, N., Xie, J., Zhao, J., Wei, M., 2021. Enhanced enzymatic hydrolysis and structure properties of bamboo by moderate two-step pretreatment. Appl. Biochem. Biotechnol. 193, 1011–1022. https://doi.org/10.1007/s12010-020-03472-x.

Yelle, D.J., Ralph, J., Lu, F., Hammel, K.E., 2008. Evidence for cleavage of lignin by a brown rot basidiomycete. Environ. Microbiol. 10, 1844–1849. https://doi.org/10.1111/j.1462-2920.2008.01605.x.

Yu, W., Wang, Y., 2023. Research on the change in chemical composition and fungal resistance of moso bamboo with heat treatment. Polymers 15, 453. https://doi.org/10.3390/polym15020453.

Zhang, J.-G., Li, Q.-L., Wei, Z.-J., 2017b. Degradation of bamboo-shoot shell powder by a fungal consortium: Changes in chemical composition and physical structure. Int. Biodeterior. Biodegrad. 116, 205–210. https://doi.org/10.1016/j.ibiod.2016.11.002.

Zhang, J.-G., Li, Q.-L., Wei, Z.-J., 2017a. Degradation of bamboo-shoot shell powder by a fungal consortium: changes in chemical composition and physical structure. Int. Biodeter. Biodegr. 116, 205–210. https://doi.org/10.1016/j.ibiod.2016.11.002.

Zhao, B., Al Rasheed, H., Ali, I., Hu, S., 2021. Efficient enzymatic saccharification of alkaline and ionic liquid-pretreated bamboo by highly active extremozymes produced by the co-culture of two halophilic fungi. Bioresour. Technol. 319, 124115. https://doi.org/10.1016/j.biortech.2020.124115.

Zhao, B., Deng, J., Liu, R., Xu, G., Cao, Y., Hu, S., 2025. Construction of a co-culture consortium for the effective degradation of bamboo lignin and its potential application in seedling substrate. Ind. Crop Prod. 225, 120589. https://doi.org/10.1016/j.indcrop.2025.120589.

Zhou, H., Wen, D., Hao, X., Chen, C., Zhao, N., Ou, R., Wang, Q., 2023. Nanostructured multifunctional wood hybrids fabricated via in situ mineralization of zinc borate in hierarchical wood structures. Chem. Eng. J. 451, 138308. https://doi.org/10.1016/j.cej.2022.138308.